

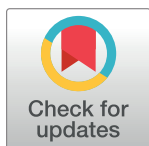
RESEARCH ARTICLE

A new CUSUM control chart under uncertainty with applications in petroleum and meteorology

Muhammad Aslam^{1*}, Ambreen Shafqat², Mohammed Albassam¹, Jean-Claude Malela-Majika³, Sandile C. Shongwe⁴

1 Department of Statistics, Faculty of Science, King Abdulaziz University, Jeddah, Saudi Arabia, **2** Department of Statistics and Financial Mathematics, Nanjing University of Science and Technology, Nanjing, Jiangsu, P.R. China, **3** Department of Statistics, Faculty of Natural and Agricultural Sciences, University of Pretoria, Hatfield, South Africa, **4** Department of Statistics, College of Science, Engineering and Technology, University of South Africa, Pretoria, South Africa

* aslam_ravian@hotmail.com, malbassam@kau.edu.sa



Abstract

In these last few decades, control charts have received a growing interest because of the important role they play by improving the quality of the products and services in industrial and non-industrial environments. Most of the existing control charts are based on the assumption of certainty and accuracy. However, in real-life applications, such as weather forecasting and stock prices, operators are not always certain about the accuracy of an observed data. To efficiently monitor such processes, this paper proposes a new cumulative sum (CUSUM) \bar{X} chart under the assumption of uncertainty using the neutrosophic statistic (NS). The performance of the new chart is investigated in terms of the neutrosophic run length properties using the Monte Carlo simulations approach. The efficiency of the proposed neutrosophic CUSUM (NCUSUM) \bar{X} chart is also compared to the one of the classical CUSUM \bar{X} chart. It is observed that the NCUSUM \bar{X} chart has very interesting properties compared to the classical CUSUM \bar{X} chart. The application and implementation of the NCUSUM \bar{X} chart are provided using simulated, petroleum and meteorological data.

OPEN ACCESS

Citation: Aslam M, Shafqat A, Albassam M, Malela-Majika J-C, Shongwe SC (2021) A new CUSUM control chart under uncertainty with applications in petroleum and meteorology. PLoS ONE 16(2): e0246185. <https://doi.org/10.1371/journal.pone.0246185>

Editor: Dragan Pamucar, University of Defence in Belgrade, SERBIA

Received: October 31, 2020

Accepted: January 14, 2021

Published: February 4, 2021

Copyright: © 2021 Aslam et al. This is an open access article distributed under the terms of the [Creative Commons Attribution License](https://creativecommons.org/licenses/by/4.0/), which permits unrestricted use, distribution, and reproduction in any medium, provided the original author and source are credited.

Data Availability Statement: All relevant data are within the paper.

Funding: The article was funded by the Deanship of Scientific Research (DSR), King Abdulaziz University. The authors, therefore, thankful to DSR for their technical and financial supports.

Competing interests: The authors have declared that no competing interests exist.

Introduction

Control charts play an essential role in monitoring processes in the production and manufacturing sectors. Shewhart-type control charts are the most popular charts because of its simplicity and attractive sensitivity towards large shifts in the process parameters. These charts are widely applied in many fields and operations (such as manufacturing processes, health care monitoring, stock exchange, credit card, financial fraud detection, weather updates, and internet traffic flow, etc.). However, Shewhart-type charts are inefficient in detecting small to moderate process shifts. Due to this drawback, researchers have developed new control charts based on classical and adaptive sampling designs to detect small-to-moderate process shifts as quickly as possible, including large shifts. Control charts are classified into memory-type (e.g.

cumulative sum (CUSUM), exponentially weighted moving average (EWMA), etc.) and memoryless (e.g. Shewhart-type) control charts; see for instance [1]. The latter uses only the latest information of the process to compute the charting statistics, which makes it less sensitive to detect small-to-moderate shifts, but enhances its ability to detect large shifts in the process. The first (i.e. memory-type control chart) uses both current and past information to compute the charting statistics, which makes it more sensitive in detecting small-to-moderate shifts and less sensitive in detecting large shifts in the process. The CUSUM and EWMA charts are the most popular memory-type control charts. To enhance the aforementioned charts, various advanced techniques are used including the addition of run rules, the use of variable sampling interval (VSI) and variable sample size (VSS) sampling designs for adaptive charts. Among all the advanced developments in the statistical process control (SPC) field, the CUSUM chart is an efficient alternative to the Shewhart chart when it comes to the detection of small to moderate shifts, see [1].

Both memory-type and memory-less control charts are used to monitor and control the spread or location parameters in any process. The sensitivity of memory-type charts have attracted the attention of many researchers and brought many more improvements in the SPC field and management of many organizations. Due to the efficiency of the CUSUM and EWMA charts, many other control charts have been developed. Lucas and Crosier [2] incorporated a fast initial response (FIR) feature to the classical CUSUM and compared its performance to that of the classical CUSUM chart. Zhao et al. [3] developed a dual CUSUM scheme which combines two CUSUM chart to detect a small shift in a process. Li and Wang [4] proposed an adaptive CUSUM Q chart also known as the self-starting approach. Shafqat et al. [5] introduced a linear prediction model based on the double EWMA control chart for non-normal situations for monitoring the location parameter. Haq [6] and Haq et al. [7, 8] proposed the use of EWMA control charts to monitor various processes, i.e. the mean and variance using ranked set sampling and the mean under the effect of measurement errors using ranked set sampling. Sanusi et al. [9] introduced a different approach for the EWMA-based chart when supplementary information about the main variable is not constant. Some different applications of attributes and variables control charts can be found in [10, 11].

The classical Shewhart control charts cannot be used efficiently when data are collected from uncertain and random situations, or when there are inconsistencies in the collected data. Khademi and Amirzadeh [12] reported that “fuzzy data exist ubiquitously in the modern manufacturing processes”; hence, in certain monitoring environments, ‘fuzzy model’ control charts are preferred when parameters or observations are uncertain, see for instance [13]. Senturk and Erginel [14] introduced the dispersion control chart by using the fuzzy logic, and Faraz et al. [15] proposed a control chart combining uncertainty and randomness assumptions. Smarandache [16] provided an overview of the fuzzy logic and reported that the neutrosophic logic deals efficiently with indeterminacy. In [17, 18], the neutrosophic logic is used to develop the idea of the neutrosophic statistics. Neutrosophic statistics is an extension of the classical statistics that is more efficient in analyzing data from ambiguous environment. For publications on neutrosophic statistics applied in various fields of knowledge, the readers are referred to [19–21]. For non-normal processes, control charts with a fuzzy approach are discussed by [22]. Pereira et al. [23] designed a fuzzy chart for monitoring the blood components under the violation of the normality assumption. The most recent research works on control charts that use neutrosophic statistics concepts, can be found in [24–28].

At the best of the authors’ knowledge, there is no work on the CUSUM control chart under neutrosophic statistics. In this paper, the CUSUM \bar{X} control chart using the neutrosophic statistical method is proposed. Following the reports in [16, 17], it is presumed that the proposed

neutrosophic CUSUM (NCUSUM) \bar{X} chart will provide very interesting properties (i.e. will be more efficient in detecting a small shift in the process and more informative, flexible, and effective in uncertain conditions).

The rest of this paper is structured as follows: The second section gives a brief description of the classical CUSUM \bar{X} chart and an introduction to the NCUSUM \bar{X} control chart. In the third section, the performance of the proposed NCUSUM \bar{X} chart is extensively investigated in terms of the neutrosophic run length properties. Moreover, the performance of the proposed chart is compared with the classical CUSUM \bar{X} chart. Fourth and fifth sections provide illustrative applications of the new chart using simulated and real-life datasets, respectively. The conclusion and recommendations are given in the last section.

The CUSUM control chart

The classical CUSUM chart. The CUSUM \bar{X} chart for monitoring small and moderate shifts in the mean was first introduced by [29]. The two-sided CUSUM chart is used to monitor upwards and downward shifts in the process parameters using the charting statistics C_i^+ and C_i^- , respectively, where i represents the sample number (or sampling time). Assume that X is a sequence of independent normally distributed observations given that the in-control mean μ_0 and variance σ_0^2 ; thus, the charting statistics of the two-sided CUSUM \bar{X} chart (i.e. C_i^+ and C_i^- , with $C_0^+ = C_0^- = 0$) are plotted versus a single control limit denoted by H . These charting statistics are mathematically defined by

$$\begin{cases} C_i^+ = \max[0, \bar{X}_i - (\mu_0 + K) + C_{i-1}^+] \\ C_i^- = \max[0, (\mu_0 - K) - \bar{X}_i + C_{i-1}^-] \end{cases} \tag{1}$$

where \bar{X} is the sample mean, μ_0 is the target mean value of X and K is the reference value. The CUSUM chart depends on two singleton parameters, i.e. K and H , which need to be selected carefully because the sensitivity of the CUSUM chart depend on them, see pages 404–405 of Montgomery [1]. These parameters are chosen such that:

$$K = k\sqrt{Var(\bar{X})} \text{ and } H = h\sqrt{Var(\bar{X})}, \tag{2}$$

where $Var(\bar{X}) = \sigma_x^2/n$, σ_x^2 is the variance of X , k is selected to be half of the shift (i.e. $k = \delta/2$, with δ is the shift in standard deviation units) and h is usually selected to be approximately five times the standard deviation units. Note that the process has moved upwards if $C_i^+ > H$ for any value of i ; however, if $C_i^- > H$, the process has moved downwards.

In the next sub-section, the proposed NCUSUM \bar{X} chart is introduced using the framework of the classical CUSUM \bar{X} chart.

The proposed neutrosophic CUSUM chart. In the uncertain environments having inconsistency data, the quality characteristic of interest (denoted by X_{Ni}) is not a deterministic value; hence, it falls within some interval, say $[X_{Li}, X_{Ui}]$, where the subscripts L and U refers to the lower and upper bound of those particular values; for instance, X_{Li} is a lower bound of X_{Ni} and X_{Ui} is the upper bound of X_{Ni} (i.e. $X_{Li} \leq X_{Ni} \leq X_{Ui}$). The latter lower and upper notation holds for other expressions defined in this subsection. That is, the neutrosophic quality characteristic of interest X_{Ni} ; $X_{Ni} \in [X_{Li}, X_{Ui}]$, follows neutrosophic normal distribution with neutrosophic mean μ_{0N} ; $\mu_{0N} \in [\mu_L, \mu_U]$ and neutrosophic variance σ_{0N}^2 ; $\sigma_{0N}^2 \in [\sigma_L^2, \sigma_U^2]$, with $\mu_L \leq \mu_U$ and $\sigma_L^2 \leq \sigma_U^2$. Hence, the sample mean of the variable X_{Ni} is given by $\bar{X}_{Ni} \in [\bar{X}_{Li}, \bar{X}_{Ui}]$, $Var(\bar{X}_{Ni}) = \sigma_{Ni}^2/n_N$; $n_N \in [n_L, n_U]$ with $n_L \leq n_U$, $\sigma_{Ni} \in [\sigma_{Li}, \sigma_{Ui}]$ is the observed neutrosophic standard deviation of X_{Ni} , with $\sigma_{Li} \leq \sigma_{Ui}$. Thus, the plotting statistics of the proposed NCUSUM

\bar{X} chart under uncertain environments is given by

$$\begin{cases} M_{Ni}^+ = \max[0, \bar{X}_{Ni} - (\mu_{0N} + K_N) + M_{N(i-1)}^+] \\ M_{Ni}^- = \max[0, (\mu_{0N} - K_N) - \bar{X}_{Ni} + M_{N(i-1)}^-] \end{cases} \quad (3)$$

where $M_{Ni}^+ \in [M_{Li}^+, M_{Ui}^+]$, $M_{Ni}^- \in [M_{Li}^-, M_{Ui}^-]$, $K_N \in [K_L, K_U]$, $H_N \in [H_L, H_U]$ and μ_{0N} is the target mean value. In addition, $\mu_{1N} = \mu_{0N} + \delta\sigma_{0N}$, where $\mu_{0N} \in [\mu_{0L}, \mu_{0U}]$ and $\mu_{1N} \in [\mu_{1L}, \mu_{1U}]$ represents the in-control and out-of-control neutrosophic mean, respectively; with δ denoting the shift in the mean. Moreover,

$$K_N = k_N \sqrt{\text{Var}(\bar{X}_N)} \text{ and } H_N = h_N \sqrt{\text{Var}(\bar{X}_N)}; k_N \in [k_L, k_U]; h_N \in [h_L, h_U], \quad (4)$$

where k_N and h_N are the design parameters of the proposed NCUSUM \bar{X} chart. The initial values for the plotting statistics which are given in Eq (3) are equal to zero, i.e. $M_{N0}^+ = M_{N0}^- = 0$. The plotting statistics of the proposed chart are plotted versus the control limit H_N . The evaluation rule for the proposed chart is given as: for any value of i , if the value of $M_{Ni}^+ > H_N$ then the process of the mean is declared to have shifted upward; otherwise, if the value of $M_{Ni}^- > H_N$ then the process mean is declared to have moved downward. The values of k_N and h_N need to be selected with caution because the run length (RL) properties of the chart depend on them. Note that the RL is the number of charting statistics that are required before the first out-of-control signal is issued by a control chart. The manner in which the design parameters k_N and h_N are obtained is discussed in the next section.

Run length performance

Performance of the NCUSUM \bar{X} chart. For some selected values of k_N and n_N , for example $k_N \in \{[0.20, 0.25], [0.4, 0.5]\}$, and $n_N \in \{[3, 5], [10, 20]\}$, the corresponding values of h_N are found by running 10^5 simulations in R software for some given fixed nominal neutrosophic average RL (denoted by $NARL_0$) values of 300, 370, 400, 500. Tables 1–3 display the in-control and out-of-control neutrosophic average and standard deviation of the RL (denoted as $NARL$ and $NSDRL$) profiles of the proposed chart using different parameters, where $NARL \in [NARL_L, NARL_U]$ and $NSDRL \in [NSDRL_L, NSDRL_U]$, with $NARL_L \leq NARL_U$ and $NSDRL_L \leq NSDRL_U$. In other words, Tables 1–3 give the ideal combinations of h_N and k_N when the nominal $NARL_0$ values are 300, 370, 400 and 500 for different values of n_N .

The following algorithm was applied to determine the values of k_N and n_N .

Step-1: specify the values of $NARL_0$ and n_N .

Step-2: Determine the values of k_N and n_N where $NARL \geq NARL_0$. Chose the values of k_N and n_N where $NARL$ is very close or exact to $NARL_0$.

Step-3: Determine the values of $NARL$ s and $NSDRL$ s for various values of δ .

The performance of the proposed NCUSUM \bar{X} control chart is evaluated in terms of different RL criteria, i.e. $NARL$ s, $NSDRL$ and the percentiles of the run length (PRL), i.e. the 25th, 50th and 75th percentiles which are denoted by $P25$ (i.e. $P25 \in [P25_L, P25_U]$), $P50$ (i.e. $P50 \in [P50_L, P50_U]$) and $P75$ (i.e. $P75 \in [P75_L, P75_U]$). The following analysis would be noticed through Tables 1–6:

1. Tables 1–5 show that there are inverse relationships between the values of out-of-control $NARL$ (denoted as $NARL_1$) and the values of δ . That is, the smallest value of $NARL_1$ is found at the largest values of δ , i.e. [1.00, 1.00]. In other words, as δ increase, the values of

Table 1. The NARL and NSDRL values of the proposed NCUSUM \bar{X} chart when $n_N \in [3, 5]$, $k_N \in [0.20, 0.25]$ for different nominal NARL.

NARL	300		370		400		500	
h_N	[7.602,8.662]		[8.099,9.299]		[8.319,9.499]		[9.039,10.299]	
δ	NARLs	NSDRLs	NARLs	NSDRLs	NARLs	NSDRLs	NARLs	NSDRLs
0	[301.07,301.18]	[271.92,283.10]	[370.28,371.70]	[330.58,342.12]	[400.39,401.79]	[360.15,371.83]	[500.44,501.54]	[441.99,447.12]
0.25	[22.74,32.70]	[12.50,19.00]	[24.94,35.23]	[13.38,20.73]	[25.64,36.61]	[13.68,20.68]	[27.04,40.06]	[14.01,22.71]
0.5	[9.11,13.77]	[3.38,5.35]	[9.77,14.57]	[3.32,5.38]	[10.20,15.04]	[3.49,5.47]	[11.15,15.74]	[3.61,5.58]
0.75	[5.00,8.59]	[1.61,2.56]	[6.36,9.33]	[1.75,2.80]	[6.54,9.52]	[1.77,2.66]	[6.96,10.14]	[1.76,2.78]
1	[4.24,6.27]	[1.06,1.60]	[4.68,6.67]	[1.09,1.69]	[4.82,6.87]	[1.06,1.71]	[5.20,7.36]	[1.15,1.71]
1.5	[2.99,4.21]	[0.58,0.87]	[3.17,4.51]	[0.57,0.87]	[3.24,4.51]	[0.61,0.89]	[3.44,4.86]	[0.61,0.91]
2	[2.25,3.22]	[0.44,0.57]	[2.44,3.38]	[0.50,0.60]	[2.46,3.42]	[0.51,0.59]	[2.67,3.70]	[0.51,0.60]
2.5	[1.99,2.60]	[0.33,0.51]	[2.03,2.81]	[0.29,0.56]	[2.03,2.84]	[0.20,0.56]	[2.14,3.03]	[0.34,0.49]
3	[1.87,2.18]	[0.15,0.38]	[1.96,2.29]	[0.19,0.45]	[1.96,2.38]	[0.17,0.46]	[1.99,2.60]	[0.29,0.39]
4	[1.15,1.97]	[0.16,0.35]	[1.26,1.99]	[0.08,0.43]	[1.36,2.00]	[0.09,0.44]	[1.62,2.01]	[0.18,0.30]
5	[1.00,1.57]	[0.00,0.29]	[1.00,1.80]	[0.03,0.39]	[1.00,1.85]	[0.05,0.40]	[1.02,1.96]	[0.15,0.25]
6	[1.00,1.07]	[0.00,0.16]	[1.00,1.20]	[0.00,0.20]	[1.00,1.22]	[0.01,0.22]	[1.00,1.55]	[0.00,0.23]
7	[1.00,1.00]	[0.00,0.03]	[1.00,1.00]	[0.00,0.07]	[1.00,1.00]	[0.00,0.09]	[1.00,1.03]	[0.00,0.12]

<https://doi.org/10.1371/journal.pone.0246185.t001>

NARL₁ decrease until they approach a value of one, i.e. [1.00,1.00]. The latter implies that, for large values of δ , the control chart will give an out-of-control signal on the next sampling point. Similarly, the NSDRLs tend to zero for largest values of δ , i.e. [0.00,0.00], which means that the variability is reduced when δ values are large.

- For a specified neutrosophic sample size, n_N , there is an increasing trend in NARL₁ values as the neutrosophic value of k_N increase at small shifts of δ ; however, there is an decreasing trend in NARL₁ values for large shifts of δ (see Tables 1 and 2). For instance, when $k_N \in [0.20, 0.25]$, $n_N \in [3, 5]$ and $\delta = 0.25$ for a NARL₀ = 370, the NARL₁ $\in [24.94, 35.23]$; however, when $k_N \in [0.40, 0.50]$, the NARL₁ $\in [28.53, 41.29]$ using the same parameters. Note though, at $\delta = 3$ for the same NARL₀ value, the NARL₁ is equal to [1.96, 2.29] and [1.08, 1.82]

Table 2. The NARL and NSDRL values of the proposed NCUSUM \bar{X} chart when $n_N \in [3, 5]$, $k_N \in [0.4, 0.5]$ for different nominal NARL.

NARL ₀	300		370		400		500	
h_N	[4.585,5.421]		[4.787,5.751]		[4.887,5.894]		[5.179,6.314]	
δ	NARLs	NSDRLs	NARLs	NSDRLs	NARLs	NSDRLs	NARLs	NSDRLs
0	[301.20,301.83]	[292.12,299.37]	[370.88,371.32]	[354.69,355.21]	[400.82,401.85]	[370.48,374.30]	[501.32,501.62]	[450.81,452.90]
0.25	[25.76,35.74]	[20.24,27.67]	[28.53,41.29]	[22.35,32.16]	[28.51,43.22]	[21.76,33.36]	[31.94,48.29]	[25.25,37.55]
0.5	[8.07,12.05]	[4.07,6.65]	[8.27,12.84]	[4.07,6.84]	[8.38,13.11]	[2.98,6.43]	[9.13,13.70]	[4.53,6.49]
0.75	[4.61,6.67]	[1.74,2.60]	[4.70,7.09]	[1.69,2.72]	[4.87,7.20]	[1.77,2.68]	[5.08,7.65]	[1.78,2.91]
1	[3.27,4.79]	[0.99,1.64]	[3.35,5.06]	[0.99,1.64]	[3.41,5.15]	[1.04,1.69]	[3.55,5.46]	[1.04,1.63]
1.5	[2.17,3.04]	[0.47,0.81]	[2.24,3.15]	[0.52,0.81]	[2.25,3.28]	[0.52,0.79]	[2.35,3.51]	[0.55,0.86]
2	[1.74,2.29]	[0.45,0.51]	[1.81,2.43]	[0.40,0.53]	[1.85,2.45]	[0.40,0.55]	[1.91,2.61]	[0.36,0.58]
2.5	[1.32,1.98]	[0.32,0.46]	[1.36,2.03]	[0.32,0.48]	[1.43,2.05]	[0.30,0.32]	[1.49,2.12]	[0.30,0.37]
3	[1.04,1.74]	[0.19,0.43]	[1.08,1.82]	[0.27,0.38]	[1.08,1.86]	[0.27,0.34]	[1.15,1.93]	[0.25,0.30]
4	[1.00,1.12]	[0.00,0.33]	[1.00,1.21]	[0.00,0.20]	[1.02,1.26]	[0.00,0.30]	[1.00,1.42]	[0.09,0.19]
5	[1.00,1.00]	[0.00,0.00]	[1.00,1.00]	[0.00,0.07]	[1.00,1.01]	[0.00,0.09]	[1.00,1.02]	[0.00,0.06]
6	[1.00,1.00]	[0.00,0.00]	[1.00,1.00]	[0.00,0.00]	[1.00,1.00]	[0.00,0.00]	[1.00,1.00]	[0.00,0.00]
7	[1.00,1.00]	[0.00,0.00]	[1.00,1.00]	[0.00,0.00]	[1.00,1.00]	[0.00,0.00]	[1.00,1.00]	[0.00,0.00]

<https://doi.org/10.1371/journal.pone.0246185.t002>

Table 3. The NARL and NSDRL values of the proposed NCUSUM \bar{X} chart when $n_N \in [10, 20]$, $k_N \in [0.4, 0.5]$ for different nominal NARL.

$NARL_0$	300		370		400		500	
h_N	[5.478,7.389]		[4.804,5.730]		[4.917,5.859]		[5.224,6.172]	
δ	NARLs	NSDRLs	NARLs	NSDRLs	NARLs	NSDRLs	NARLs	NSDRLs
0	[301.10,301.60]	[282.31,301.61]	[370.27,370.54]	[353.60,359.17]	[401.29,401.47]	[374.27,385.41]	[500.08,501.92]	[453.29,460.42]
0.25	[12.32,13.55]	[3.84,6.87]	[8.43,14.49]	[4.28,8.06]	[8.50,14.96]	[4.02,7.65]	[9.09,15.13]	[4.12,7.73]
0.5	[4.89,5.46]	[0.97,1.80]	[3.45,5.51]	[1.06,1.94]	[3.47,5.65]	[1.01,1.88]	[3.67,6.11]	[1.08,2.07]
0.75	[3.16,3.29]	[0.49,0.94]	[2.23,3.50]	[0.51,0.90]	[2.27,3.62]	[0.49,0.96]	[2.39,3.74]	[0.56,0.99]
1	[2.32,2.86]	[0.45,0.61]	[1.81,2.67]	[0.41,0.61]	[1.84,2.68]	[0.40,0.64]	[1.92,2.79]	[0.33,0.65]
1.5	[1.63,1.87]	[0.23,0.34]	[1.08,1.95]	[0.27,0.37]	[1.09,1.94]	[0.28,0.58]	[1.17,2.00]	[0.25,0.37]
2	[1.02,1.14]	[0.00,0.27]	[1.00,1.41]	[0.03,0.25]	[1.00,1.49]	[0.00,0.50]	[1.00,1.58]	[0.00,0.49]
2.5	[1.00,1.00]	[0.00,0.14]	[1.00,1.06]	[0.00,0.20]	[1.00,1.04]	[0.00,0.20]	[1.00,1.09]	[0.00,0.28]
3	[1.00,1.00]	[0.00,0.00]	[1.00,1.00]	[0.00,0.03]	[1.00,1.00]	[0.00,0.04]	[1.00,1.00]	[0.00,0.03]
4	[1.00,1.00]	[0.00,0.00]	[1.00,1.00]	[0.00,0.00]	[1.00,1.00]	[0.00,0.00]	[1.00,1.00]	[0.00,0.00]
5	[1.00,1.00]	[0.00,0.00]	[1.00,1.00]	[0.00,0.00]	[1.00,1.00]	[0.00,0.00]	[1.00,1.00]	[0.00,0.00]
6	[1.00,1.00]	[0.00,0.00]	[1.00,1.00]	[0.00,0.00]	[1.00,1.00]	[0.00,0.00]	[1.00,1.00]	[0.00,0.00]
7	[1.00,1.00]	[0.00,0.00]	[1.00,1.00]	[0.00,0.00]	[1.00,1.00]	[0.00,0.00]	[1.00,1.00]	[0.00,0.00]

<https://doi.org/10.1371/journal.pone.0246185.t003>

for k_N equal to [0.20,0.25] and [0.40,0.50], respectively. Moreover, when design parameters are kept fixed, as δ increase, there is a decrease in the values of $NARL_1$.

- From Tables 2 and 3, it can be noticed that the $NARL_1$ decreases rapidly when n_N increase, with the restriction for the value of $[k_L, k_U]$ being constant. For instance, when $\delta = 0.25$ and $[k_L, k_U] = [0.40,0.50]$ for a nominal $NARL_0 = 370$, the $NARL_1$ is equal to [28.53,41.29] and [8.43,14.49] when n_N is equal to [3,5] and [10,20], respectively. This indicates improving detection ability.
- The in-control neutrosophic RL distribution of the proposed chart is positively skewed as the in-control $NARL$ are greater than the in-control $P50$. For instance, for the design parameters $k_N \in [0.20,0.25]$ and $n_N \in [3,5]$ corresponding to $\delta = 0$, the in-control values of

Table 4. The neutrosophic percentile points of the proposed NCUSUM \bar{X} chart when $n_N \in [3, 5]$, $k_N \in [0.20, 0.25]$ for different nominal NARL.

$NARL_0$	300		370		400		500	
δ	P25	P50	P25	P75	P50	P75	P25	P50
0	[98,104]	[220,230]	[111,123]	[399,420]	[273,277]	[502,518]	[119,132]	[293,294]
0.25	[14,19]	[21,28]	[15,21]	[28,41]	[22,30]	[31,44]	[16,22]	[23,31]
0.5	[7,10]	[9,13]	[7,11]	[11,17]	[9,14]	[12,18]	[8,11]	[10,14]
0.75	[5,7]	[6,8]	[5,7]	[7,10]	[6,9]	[7,11]	[5,8]	[6,9]
1	[4,5]	[4,6]	[4,5]	[5,7]	[5,6]	[5,8]	[4,6]	[5,7]
1.5	[3,4]	[3,4]	[3,4]	[3,5]	[3,4]	[3,5]	[3,4]	[3,4]
2	[2,3]	[2,3]	[2,3]	[3,4]	[2,3]	[3,4]	[2,3]	[2,3]
2.5	[2,2]	[2,3]	[2,3]	[2,3]	[2,3]	[2,3]	[2,3]	[2,3]
3	[2,2]	[2,2]	[2,2]	[2,2]	[2,2]	[2,3]	[2,2]	[2,2]
4	[1,2]	[1,2]	[1,2]	[1,2]	[1,2]	[2,2]	[1,2]	[1,2]
5	[1,1]	[1,2]	[1,2]	[1,2]	[1,2]	[1,2]	[1,2]	[1,2]
6	[1,1]	[1,1]	[1,1]	[1,1]	[1,1]	[1,1]	[1,1]	[1,1]
7	[1,1]	[1,1]	[1,1]	[1,1]	[1,1]	[1,1]	[1,1]	[1,1]

<https://doi.org/10.1371/journal.pone.0246185.t004>

Table 5. The neutrosophic percentile points of the proposed NCUSUM \bar{X} chart when $n_N \in [3, 5]$, $k_N \in [0.4, 0.5]$ for different nominal NARL.

NARL ₀	300		370		400		500	
	P25	P50	P25	P75	P50	P75	P25	P50
0	[87,91]	[201,202]	[109,109]	[405,428]	[264,268]	[504,528]	[120,120]	[285,293]
0.25	[12,17]	[19,27]	[12,18]	[34,47]	[22,33]	[37,54]	[13,19]	[22,33]
0.5	[5,7]	[7,10]	[5,8]	[10,15]	[7,11]	[10,16]	[6,8]	[7,12]
0.75	[3,5]	[4,6]	[3,5]	[6,8]	[4,7]	[6,8]	[4,5]	[5,7]
1	[3,4]	[3,5]	[3,4]	[4,6]	[3,5]	[4,6]	[3,4]	[3,5]
1.5	[2,3]	[2,3]	[2,3]	[2,3]	[2,3]	[3,4]	[2,3]	[2,3]
2	[1,2]	[2,2]	[2,2]	[2,3]	[2,2]	[2,3]	[2,2]	[2,2]
2.5	[1,2]	[1,2]	[1,2]	[2,2]	[1,2]	[2,2]	[1,2]	[1,2]
3	[1,1]	[1,2]	[1,2]	[1,2]	[1,2]	[1,2]	[1,2]	[1,2]
4	[1,1]	[1,1]	[1,1]	[1,1]	[1,1]	[1,1]	[1,1]	[1,1]
5	[1,1]	[1,1]	[1,1]	[1,1]	[1,1]	[1,1]	[1,1]	[1,1]
6	[1,1]	[1,1]	[1,1]	[1,1]	[1,1]	[1,1]	[1,1]	[1,1]
7	[1,1]	[1,1]	[1,1]	[1,1]	[1,1]	[1,1]	[1,1]	[1,1]

<https://doi.org/10.1371/journal.pone.0246185.t005>

the $P50 \in [273,277]$ are smaller than $NARL_0 = 370$ (see for instance Tables 1–6). The latter implies that the distribution of the NCUSUM \bar{X} chart is positively skewed.

- Regardless of the $NARL_0$ value, the sensitivity of the NCUSUM \bar{X} chart increase rapidly as δ increases in terms of the P25, P50 and P75 values, see Tables 4–6.

Comparison of the proposed NCUSUM \bar{X} and classical CUSUM \bar{X} charts. The persistent need for more awareness of the proposed NCUSUM \bar{X} chart, comprehensive comparison has been made with classical CUSUM \bar{X} chart. To get valid deductions, the in-control ARLs of both charts are set at nominal levels of 370 and 500, and the performance is compared in terms of the out-of-control ARLs and SDRLs. The strategy of working in this section is parallel to [27], that is, a control chart under neutrosophic design is said to be capable if it has smaller NARL values compared to its counterpart. Thus, the efficiency of the proposed chart in terms

Table 6. The neutrosophic percentile points of the proposed NCUSUM \bar{X} chart when $n_N \in [10, 20]$, $k_N \in [0.4, 0.5]$ for different nominal NARL.

NARL ₀	300		370		400		500	
	P25	P50	P25	P75	P50	P75	P25	P50
0.00	[89,90]	[201,205]	[111,114]	[408,408]	[250,251]	[511,547]	[120,121]	[275,276]
0.25	[5,8]	[7,12]	[5,9]	[10,17]	[8,12]	[10,18]	[6,9]	[8,13]
0.5	[3,4]	[3,5]	[3,4]	[4,6]	[3,5]	[4,6]	[3,4]	[3,5]
0.75	[2,3]	[2,3]	[2,3]	[2,4]	[2,3]	[3,4]	[2,3]	[2,3]
1	[1,2]	[2,2]	[2,2]	[2,3]	[2,3]	[2,3]	[2,2]	[2,3]
1.5	[1,2]	[1,2]	[1,2]	[1,2]	[1,2]	[1,2]	[1,2]	[1,2]
2	[1,1]	[1,1]	[1,1]	[1,2]	[1,1]	[1,2]	[1,1]	[1,1]
2.5	[1,1]	[1,1]	[1,1]	[1,1]	[1,1]	[1,1]	[1,1]	[1,1]
3	[1,1]	[1,1]	[1,1]	[1,1]	[1,1]	[1,1]	[1,1]	[1,1]
4	[1,1]	[1,1]	[1,1]	[1,1]	[1,1]	[1,1]	[1,1]	[1,1]
5	[1,1]	[1,1]	[1,1]	[1,1]	[1,1]	[1,1]	[1,1]	[1,1]
6	[1,1]	[1,1]	[1,1]	[1,1]	[1,1]	[1,1]	[1,1]	[1,1]
7	[1,1]	[1,1]	[1,1]	[1,1]	[1,1]	[1,1]	[1,1]	[1,1]

<https://doi.org/10.1371/journal.pone.0246185.t006>

Table 7. Comparison of the NCUSUM and the classical CUSUM (CCUSUM) \bar{X} charts when $k = 0.5, k_N \in [0.4, 0.5]$.

δ	CCUSUM chart: $ARL_0 = 370$		NCUSUM chart: $NARL_0 = 370$		CCUSUM chart: $ARL_0 = 500$		NCUSUM chart: $NARL_0 = 500$	
	$h = 4.822$		$n_N \in [3, 5], h_N \in [4.887, 5.894]$		$h = 5.296$		$n_N \in [3, 5], h_N \in [5.224, 6.172]$	
	ARLs	SDRLs	NARLs	NSDRLs	ARLs	SDRLs	NARLs	NSDRLs
0	370.11	354.62	[370.88,371.32]	[354.69,355.21]	500.86	458.86	[501.32,501.62]	[501.32,501.62]
0.25	125.27	122.52	[28.53,41.29]	[22.35,32.16]	162.99	150.86	[31.94,48.29]	[48.29,31.94]
0.5	35.37	28.00	[8.27,12.84]	[4.07,6.84]	43.01	33.77	[9.13,13.70]	[13.70,9.13]
0.75	16.39	10.48	[4.70,7.09]	[1.69,2.72]	18.15	11.89	[5.08,7.65]	[7.65,5.08]
1	9.98	5.25	[3.35,5.06]	[0.99,1.64]	11.46	6.37	[3.55,5.46]	[5.46,3.55]
1.5	5.60	2.18	[2.24,3.15]	[0.52,0.81]	5.96	2.19	[2.35,3.51]	[3.51,2.35]
2	3.85	1.23	[1.81,2.43]	[0.40,0.53]	4.19	1.27	[1.91,2.61]	[2.61,1.91]
2.5	3.00	0.85	[1.36,2.03]	[0.32,0.48]	3.26	0.89	[1.49,2.12]	[2.12,1.49]
3	2.48	0.63	[1.08,1.82]	[0.27,0.38]	2.72	0.71	[1.15,1.93]	[1.93,1.15]
4	1.95	0.37	[1.00,1.21]	[0.00,0.20]	2.07	0.38	[1.00,1.42]	[1.42,1.00]
5	1.62	0.48	[1.00,1.00]	[0.00,0.07]	1.80	0.40	[1.00,1.02]	[1.02,1.00]
6	1.24	0.43	[1.00,1.00]	[0.00,0.00]	1.40	0.49	[1.00,1.00]	[1.00,1.00]
7	1.04	0.19	[1.00,1.00]	[0.00,0.00]	1.11	0.31	[1.00,1.00]	[1.00,1.00]

<https://doi.org/10.1371/journal.pone.0246185.t007>

of the *NARL* values is compared to the *ARL* values of the classical CUSUM \bar{X} chart. For instance, the classical CUSUM \bar{X} chart with parameters $k = 0.5$ and $h = 4.822$ identifies a shift of size equal to 0.25 after 125.27 charting statistics for an *ARL*₀ of 370; however, the proposed NCUSUM \bar{X} chart with parameters $k_N \in [0.4, 0.5]$ and $h_N \in [4.887, 5.894]$ identifies a shift of size equal to 0.25 between the interval [28.53,41.29] samples for an *NARL*₀ of 370. In general, the comparison in Table 7 indicates that for small, moderate and large shifts in the process mean, the *NARL* and *NSDRL* are smaller in magnitude as compared to the *ARL* and *SDRL* of the classical chart, at each corresponding shift value; and thus, the proposed NCUSUM \bar{X} chart performs better than the classical CUSUM \bar{X} chart. In summary, the neutrosophic and classical *ARL*s and *SDRL*s of the NCUSUM and CUSUM \bar{X} charts indicate that the NCUSUM \bar{X} chart has the higher shift detection ability as compared to the classical CUSUM \bar{X} chart.

Application of the NCUSUM \bar{X} chart using simulated data

In this section, the performance of the NCUSUM \bar{X} chart is compared to one of the classical CUSUM \bar{X} chart using simulated data. Fifty observations are generated using the neutrosophic normal distribution. The first twenty observations are generated by assuming that the process is statistically in-control and the next 30 observations are generated by assuming that the process has shifted with $\delta = 0.25$. The simulated data along with $n_N \in [3, 5]$, $k_N \in [0.4, 0.5]$, $h_N \in [4.887, 5.894]$, $\sigma_{0N} \in [1.00, 1.00]$, and $NARL_1 \in [28.53, 41.29]$, so the shift should be detected between the 28th and 41st samples. The results from the simulated data are displayed in Figs 1 and 2 for the proposed NCUSUM chart and the existing classical CUSUM \bar{X} chart, respectively.

From Figs 1 and 2, it can be seen that the proposed NCUSUM \bar{X} chart detects the first shift at around the 30th sample in between the 28th and 41st samples; however, the classical CUSUM \bar{X} chart indicates that all the charting statistics are in-control. Hence, it can be deduced that, the proposed NCUSUM \bar{X} chart has the ability to detect the shifts in the process mean earlier as compared to its classical counterpart. Therefore, the NCUSUM \bar{X} chart is more efficient and performs better than the classical CUSUM \bar{X} chart.

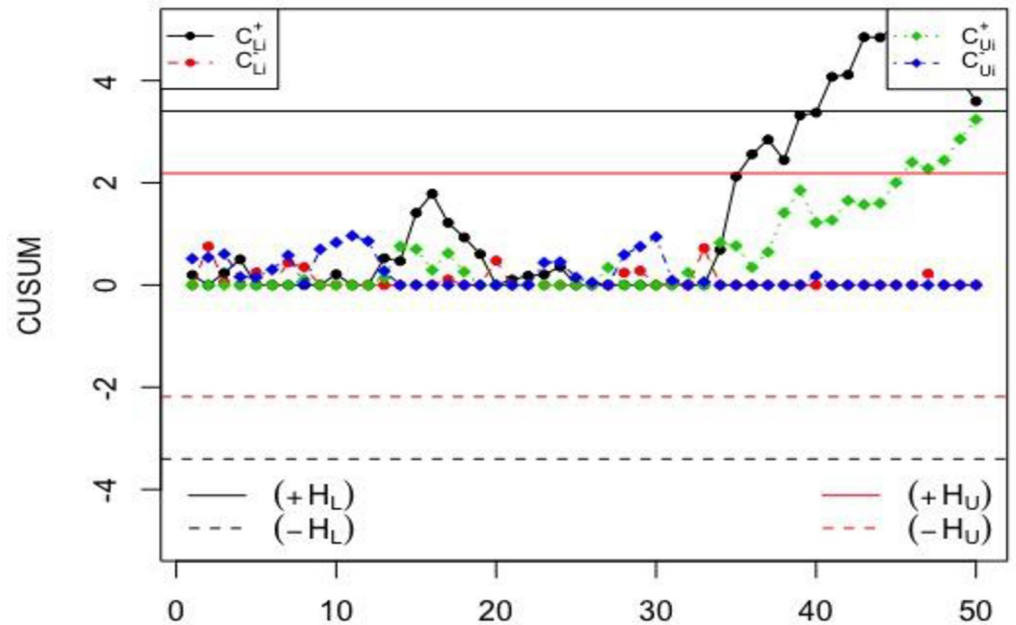


Fig 1. The proposed NCUSUM \bar{X} chart for simulated dataset.

<https://doi.org/10.1371/journal.pone.0246185.g001>

Real-data application of the proposed CUSUM \bar{X} chart

This section presents case-studies for the NCUSUM \bar{X} chart that were applied to two types of data; the first example was dedicated to the case-study on the Pakistan state oil (PSO), while the second example is the case-study on the weather forecasting. The data were taken from the Stock Exchange and Meteorological Department of Pakistan. However, as mentioned in [28], all the observations and measurements of the current variables are not crisp numbers; they are

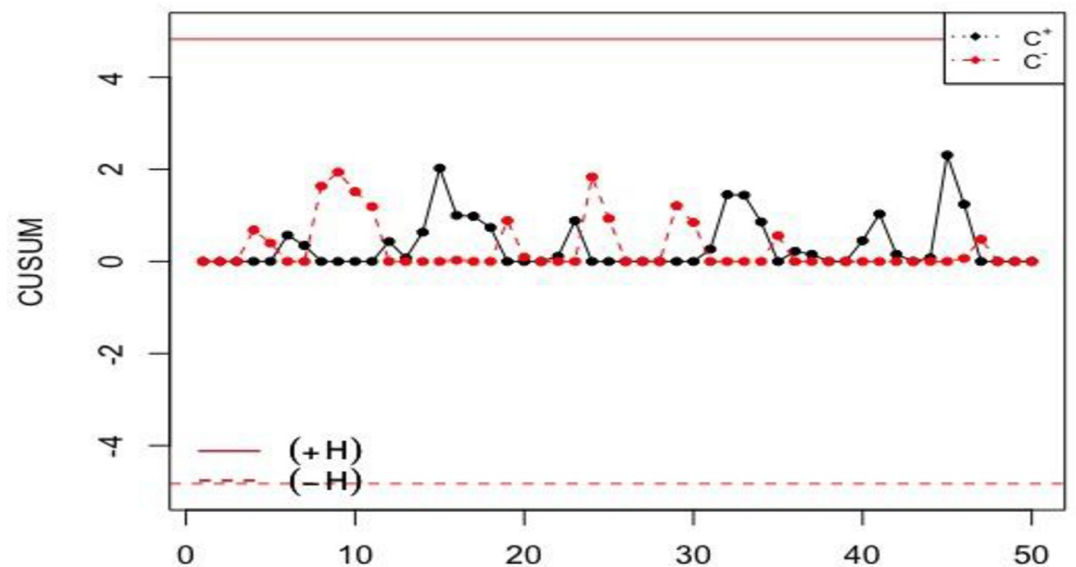


Fig 2. The classical CUSUM \bar{X} chart for simulated dataset.

<https://doi.org/10.1371/journal.pone.0246185.g002>

neutrosophically varied with some indeterminacy in representing intervals instead of singleton numbers.

Petroleum industry case-study (PSO). The oil prices are strongly related with the stock prices, which is dependent on the principle of demand and there are some indeterminacy in its measurements. The dataset in Table 8 denotes the stock price in 8 different days of August of the last 10 years for the PSO. For this data, let $n_N = 8$ and $NARL_0 = 370$. The reference value $K_N = 0.5\sigma_{0N}/\sqrt{n_N}$ (i.e. $k = 0.5$), and decision interval $H_N = h\sigma_{0N}/\sqrt{n_N}$, where $\sigma_{0N} \in [1.9221, 2.239]$, $n_N = 8$ and $h = 4.804$ are determined by using the procedure used to derive the values in Tables 1–3. Thus, the calculated decision interval and reference value given in Eq (4) is $H_N \in [3.265, 3.803]$ and $K_N \in [0.3397, 0.3958]$. The calculated charting statistics of the NCUSUM chart (i.e. M_{Ni}^+ and M_{Ni}^-) according to Eq (3) are provided in the last two columns of Table 8 and also plotted in Fig 3; however, those of the existing classical CUSUM \bar{X} chart are plotted in Fig 4.

From Fig 3, it can be noted that the PSO petroleum stock price are out-of-control in 2013 to 2015 (i.e. higher prices); while, in 2011 and 2012 the petroleum oil prices are in-control (within reasonable range). However, after 2015, the prices are decreasing and are in-control. From Fig 4, it can be seen that in all the monitored years, the PSO petroleum prices are in-control. From the comparison of both the charts, it can be seen that the proposed neutrosophic chart performs better and detects shifts earlier as compared to the classical counterpart.

Pakistan meteorological case-study. For the Meteorological Department dataset of Pakistan, the application of the proposed NCUSUM \bar{X} chart is discussed. Since weather warning is a vital forecast because it is used for protecting people's property and well-being as well as some socio-economic benefits. Thus, numerical weather experts use advanced mathematical formulas to predict the weather. Table 9 shows the weather forecast data information from 9 different cities in Pakistan for 12 months. The abbreviations symbols for the cities name are: Lahore = LHR, Karachi = KHI, Multan = MUX, Faisalabad = FSD, Islamabad = ISB, Peshawar = PEW, Hyderabad = HDD, Skardu = KDU and Gilgit = GIL.

Let the sample size and the in-control ARL values be $n_N = 12$ and $NARL_0 = 370$, while the reference and decision interval values are $H_N \in [1.4109, 2.6919]$ and $K_N \in [0.1472, 0.2809]$ when $h = 4.791$, $k = 0.5$, and $\sigma_{0N} \in [1.0197, 1.9464]$. So, the calculated NCUSUM charting statistics (i.e. M_{Ni}^+ and M_{Ni}^-) are given in the last two columns of Table 9. The charting statistics of the proposed NCUSUM \bar{X} chart are shown in Fig 5 and the ones of the classical CUSUM \bar{X} chart are shown in Fig 6.

From Fig 5, the proposed NCUSUM \bar{X} chart is found to be more efficient and gives better results compared to its classical counterpart in Fig 6; as it indicates downwards shift in the weather forecast and shows that the weather is very cold in Skardu and Gilgit cities. Note though, the classical CUSUM \bar{X} chart reveals that all cities' weather are within normal range and does not detect the shift at any point in the data. Thus, in comparison of both the control charts for monitoring weather forecasting, we can say that the NCUSUM \bar{X} chart provides better prediction especially when meteorologists are not sure about the temperature values to be used for weather prediction. Therefore, the neutrosophic CUSUM \bar{X} chart is recommended for weather prediction under the uncertainty environments.

Conclusion and future recommendations

In this paper, a new NCUSUM \bar{X} control chart is proposed. The neutrosophic run length performance of the proposed chart is computed using Monte Carlo simulations. The application of the proposed chart is illustrated using simulated data and two real-life examples using the PSO petroleum industry dataset and the weather forecasting dataset from nine cities in

Table 8. Real-life example based on the PSO petroleum company's stock price where $h = 4.804$, $k = 0.5$, $n = 8$, $H_N \in [3.265, 3.803]$, $\mu_N \in [226.897, 232.9635]$ and $\sigma_N \in [1.9221, 2.239]$.

Year	PSO petroleum oil company's stock price											$[\bar{X}_{H_i}, \bar{X}_{(H)}]$	$[M_{H_i}^+, M_{(H)}^+]$	$[M_{H_i}^-, M_{(H)}^-]$			
	AUGD10	AUGD11	AUGD12	AUGD13	AUGD17	AUGD18	AUGD19	AUGD20									
2020	[182.00,185.25]	[184.6,190.00]	[184.01,190.52]	[182.9,185.75]	[185.51,197.00]	[191.5,197.00]	[190.51,194.75]	[190.0,194.99]	[186.37,191.90]	[0.00,0.00]	[0.00,0.00]	[0.00,0.00]	[0.00,0.00]	[0.00,0.00]	[0.00,0.00]	[0.00,0.00]	[0.00,0.00]
2019	[132.0,138.01]	[132.0,138.01]	[132.0,138.01]	[132.0,138.01]	[127.26,132.00]	[127.26,132.00]	[126.25,134.24]	[132.5,137.79]	[130.16,136.01]	[0.00,0.00]	[0.00,0.00]	[0.00,0.00]	[0.00,0.00]	[0.00,0.00]	[0.00,0.00]	[0.00,0.00]	[0.00,0.00]
2018	[279.17,283.24]	[279.17,283.24]	[279.17,283.24]	[288.71,294.62]	[284.57,290.25]	[284.57,290.25]	[284.57,290.25]	[283.33,292.08]	[282.91,288.39]	[0.91,0.97]	[0.91,0.97]	[0.91,0.97]	[0.91,0.97]	[0.91,0.97]	[0.91,0.97]	[0.91,0.97]	[0.91,0.97]
2017	[318.06,329.86]	[311.11,320.83]	[311.11,320.83]	[311.11,320.83]	[304.19,311.73]	[301.04,309.38]	[301.04,309.38]	[301.04,309.38]	[307.33,316.52]	[2.53,2.59]	[2.53,2.59]	[2.53,2.59]	[2.53,2.59]	[2.53,2.59]	[2.53,2.59]	[2.53,2.59]	[2.53,2.59]
2016	[286.46,290.90]	[285.08,288.19]	[285.08,288.19]	[285.08,288.19]	[284.03,288.19]	[281.25,284.73]	[279.52,283.82]	[279.52,283.82]	[283.25,286.91]	[3.40,3.57]	[3.40,3.57]	[3.40,3.57]	[3.40,3.57]	[3.40,3.57]	[3.40,3.57]	[3.40,3.57]	[3.40,3.57]
2015	[261.81,267.08]	[263.87,267.63]	[261.81,265.28]	[256.25,264.58]	[250.83,257.64]	[252.86,256.04]	[250.38,256.25]	[244.62,250.69]	[255.31,260.64]	[3.61,3.83]	[3.61,3.83]	[3.61,3.83]	[3.61,3.83]	[3.61,3.83]	[3.61,3.83]	[3.61,3.83]	[3.61,3.83]
2014	[265.69,269.79]	[253.67,267.02]	[247.58,256.24]	[248.73,259.73]	[254.31,263.67]	[258.86,268.48]	[254.25,261.81]	[254.86,263.53]	[254.74,263.77]	[3.89,4.06]	[3.89,4.06]	[3.89,4.06]	[3.89,4.06]	[3.89,4.06]	[3.89,4.06]	[3.89,4.06]	[3.89,4.06]
2013	[228.47,244.73]	[228.47,244.73]	[244.73,251.03]	[245.87,250.63]	[240.35,245.98]	[240.35,245.98]	[237.23,249.46]	[243.23,251.03]	[238.58,247.94]	[3.77,3.87]	[3.77,3.87]	[3.77,3.87]	[3.77,3.87]	[3.77,3.87]	[3.77,3.87]	[3.77,3.87]	[3.77,3.87]
2012	[175.14,177.57]	[175.14,177.57]	[175.14,177.57]	[175.00,180.56]	[174.79,176.39]	[174.79,176.39]	[174.79,176.39]	[174.79,176.39]	[174.94,177.35]	[1.86,2.00]	[1.86,2.00]	[1.86,2.00]	[1.86,2.00]	[1.86,2.00]	[1.86,2.00]	[1.86,2.00]	[1.86,2.00]
2011	[145.94,149.97]	[148.61,157.46]	[157.64,163.19]	[157.64,163.19]	[165.01,167.71]	[160.42,165.28]	[153.92,157.23]	[153.92,157.23]	[155.38,160.15]	[0.00,0.00]	[0.00,0.00]	[0.00,0.00]	[0.00,0.00]	[0.00,0.00]	[0.00,0.00]	[0.00,0.00]	[0.00,0.00]

<https://doi.org/10.1371/journal.pone.0246185.t008>

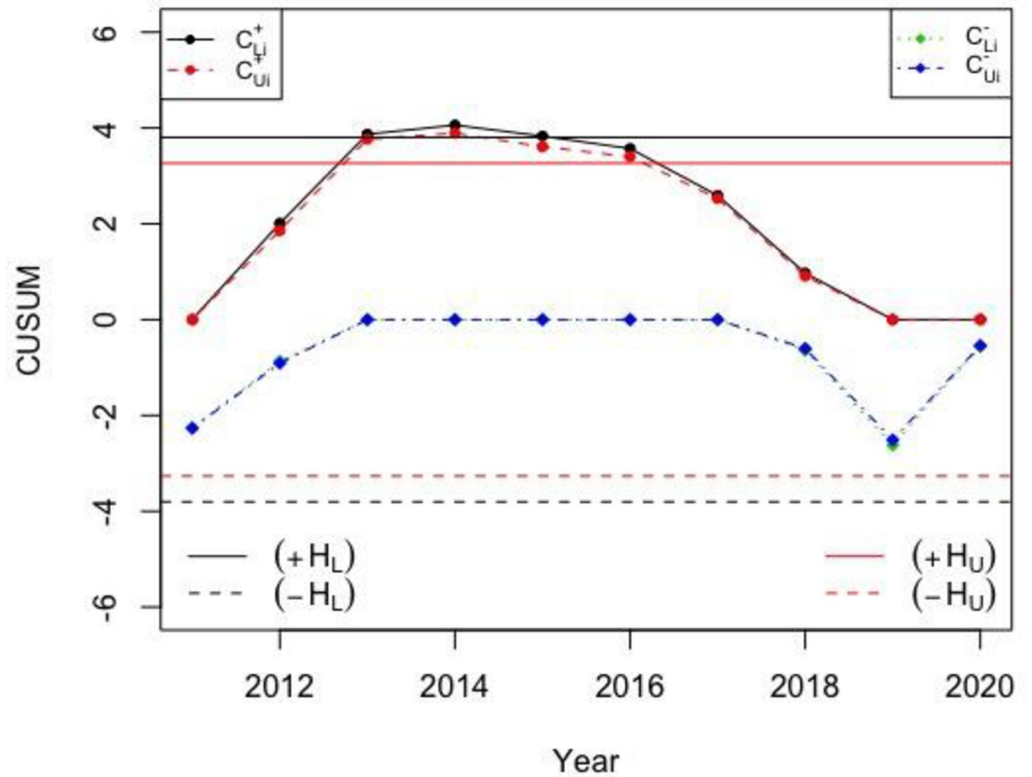


Fig 3. Real-life data from PSO petroleum oil company's stock price for the proposed NCUSUM \bar{X} chart with $H_N \in [3.265, 3.803]$ and $K_N \in [0.3397, 0.3958]$.

<https://doi.org/10.1371/journal.pone.0246185.g003>

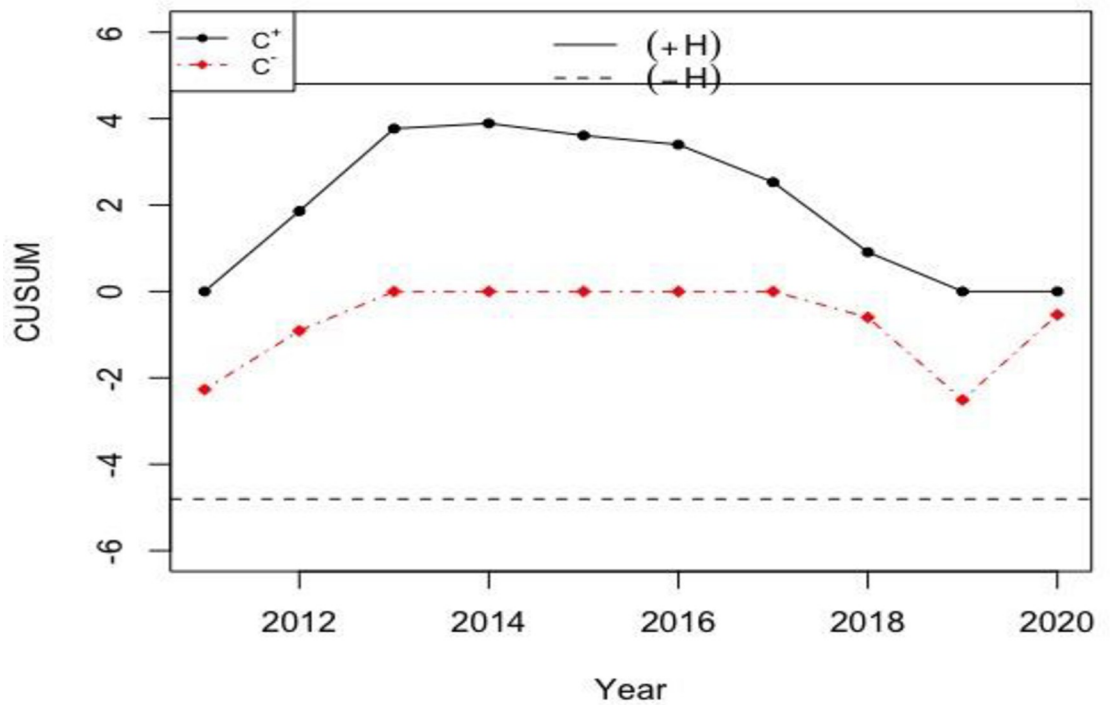


Fig 4. Real-life data from PSO petroleum company's stock price for the classical CUSUM \bar{X} chart with $h = 4.804$ and $k = 0.5$.

<https://doi.org/10.1371/journal.pone.0246185.g004>

Table 9. Meteorological department dataset for real-life example with design parameters $h = 4.791$, $H = 1.409$, $k = 0.5$ and $n = 12$.

City	Weather Update by Month												$[\bar{X}_{it}, \bar{X}_{it}]$	$[M_{it}^+, M_{it}^-]$	$[M_{it}^+, M_{it}^-]$
	Jan	Feb	Mar	April	May	Jun	July	Aug.	Sep.	Oct	Nov	Dec			
LHR	[5.9,19.8]	[8.9,22.0]	[14.0,27.1]	[19.6,33.9]	[23.7,38.6]	[27.4,40.4]	[26.9,36.1]	[26.4,35.0]	[24.4,35.0]	[18.2,32.9]	[11.6,27.4]	[6.8,21.6]	[17.81,30.81]	[0.00,0.15]	[0.00,0.00]
KHI	[10.4,25.8]	[12.7,27.7]	[17.6,31.5]	[22.3,34.3]	[25.9,35.2]	[27.9,34.8]	[27.4,33.1]	[26.1,31.7]	[25.2,32.6]	[21.34,7]	[15.9,31.9]	[11.6,27.4]	[20.35,31.72]	[0.16,0.81]	[0.00,0.00]
MUX	[4.5,21]	[7.6,23.2]	[13.5,28.5]	[19.5,35.5]	[24.4,40.4]	[28.6,42.3]	[28.7,39.2]	[28,38]	[24.9,37.2]	[18.2,34.6]	[10.9,28.5]	[5.5,22.7]	[17.85,32.61]	[0.49,0.98]	[0.00,0.00]
FSD	[4.4,19.4]	[7.4,22.4]	[12.6,27.3]	[18.1,33.8]	[23.3,38.9]	[27.4,40.7]	[27.4,37.3]	[26.9,36.3]	[24.2,36]	[17.6,33.6]	[10.4,27.5]	[5.7,21.8]	[17.11,31.25]	[0.56,0.99]	[0.00,0.00]
ISB	[2.6,17.7]	[5.1,19.1]	[9.9,23.9]	[15.30,1]	[19.7,35.3]	[23.7,38.7]	[24.3,35]	[23.5,33.4]	[20.6,33.5]	[13.9,30.9]	[7.5,25.4]	[3.4,19.7]	[14.10,28.55]	[0.13,0.42]	[0.00,0.00]
PEW	[4.18,3]	[6.3,19.5]	[11.2,23.7]	[16.4,30]	[21.3,35.9]	[25.7,40.4]	[26.6,37.7]	[25.7,35.7]	[22.7,35]	[16.1,31.2]	[7.6,25.6]	[4.9,20.1]	[15.70,29.42]	[0.00,0.16]	[0.00,0.00]
HDD	[11.1,25]	[13.6,28.1]	[18.5,33.9]	[23.38,9]	[26.2,41.6]	[28.1,40.2]	[27.8,37.4]	[26.7,36.3]	[25.3,36.8]	[22.3,37.2]	[17.3,31.9]	[12.5,26.3]	[21.03,34.46]	[0.68,0.95]	[0.00,0.00]
KDU	[-12,-3]	[-11,-1]	[-5,5]	[0,12]	[3,15]	[7,20]	[10,23]	[10,22]	[5,20]	[-1,14]	[-6,7]	[-10,0]	[-0.83,11.16]	[0.00,0.00]	[-2.72,-2.52]
GIL	[-2.7,9.6]	[0.4,12.6]	[5.4,18.4]	[9.2,24.2]	[11.8,29]	[14.9,34.2]	[18.2,36.2]	[17.5,35.3]	[12.4,31.8]	[6.3,25.6]	[0.4,18.4]	[-2.3,11.6]	[7.62,23.91]	[0.00,0.00]	[-3.45,-3.02]

<https://doi.org/10.1371/journal.pone.0246185.t009>

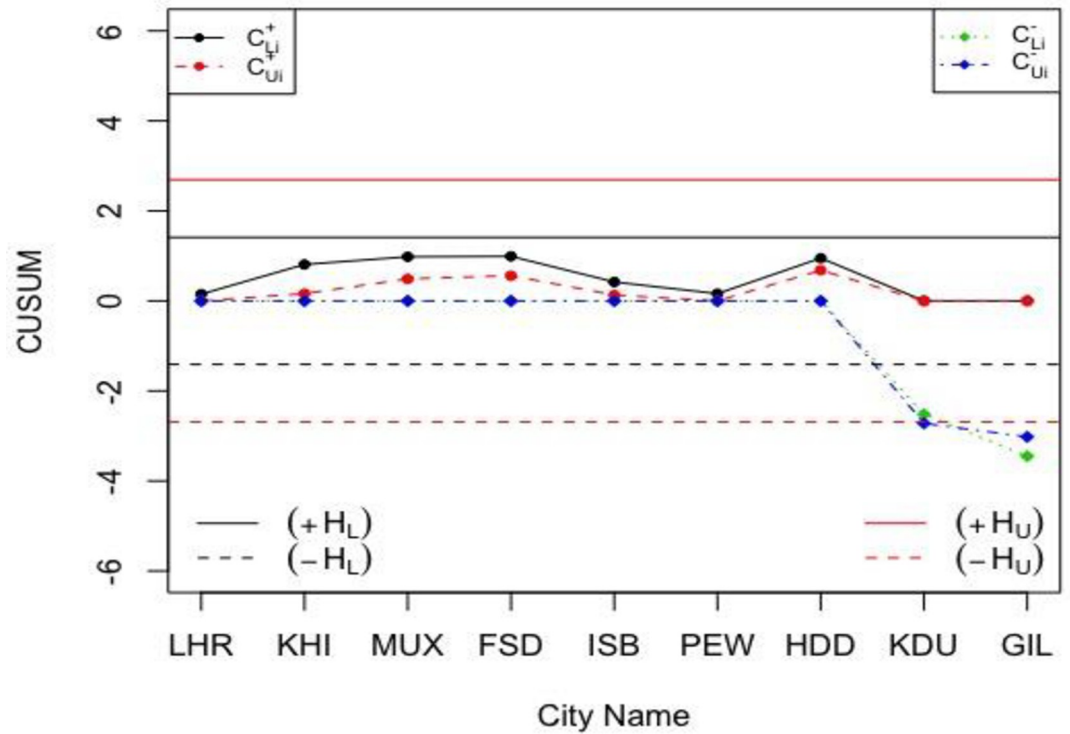


Fig 5. The proposed NCUSUM \bar{X} chart for the weather condition in Pakistan with $H_N \in [1.4109, 2.6919]$ and $K_N \in [0.1472, 0.2809]$.

<https://doi.org/10.1371/journal.pone.0246185.g005>

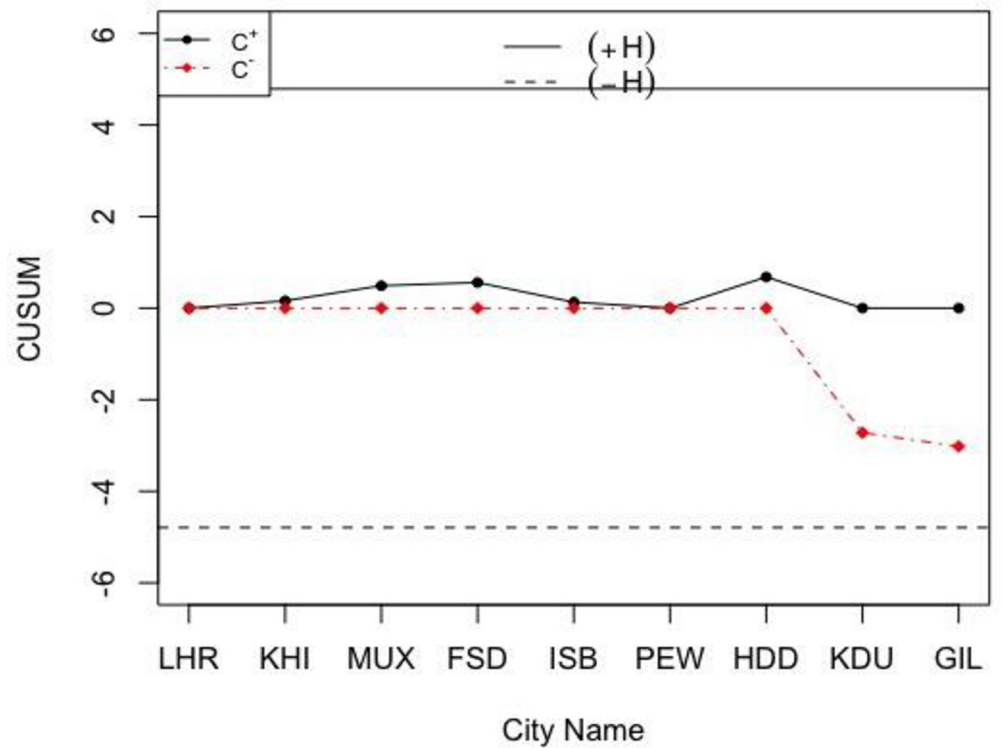


Fig 6. The classical CUSUM \bar{X} chart for the weather data with $h = 4.791$ and $k = 0.5$.

<https://doi.org/10.1371/journal.pone.0246185.g006>

Pakistan. The results show that the NCUSUM \bar{X} chart is better suited for use than the classical CUSUM \bar{X} chart either when the data are inaccurate or when the operators do not have a complete dataset or for uncertain environments situations. The comparison study shows that the proposed neutrosophic chart is efficient in detecting small to large shifts in the process parameter than the classical chart. Note that the NCUSUM \bar{X} chart is functional when the variable of interest adopts the neutrosophic normal distribution. The proposed neutrosophic chart is also recommended for monitoring the process mean shifts for the medical instruments, automobiles, aerospace and drinking water industries.

Further future works can be dedicated to the NCUSUM \bar{X} chart that can be designed for non-normal distributions, as well as for the multiple dependent state sampling and repetitive sampling approaches.

Acknowledgments

The authors are deeply thankful to the editor and reviewers for their valuable suggestions to improve the quality of the original manuscript.

Author Contributions

Data curation: Ambreen Shafqat.

Funding acquisition: Mohammed Albassam.

Software: Ambreen Shafqat.

Supervision: Muhammad Aslam.

Visualization: Mohammed Albassam.

Writing – original draft: Muhammad Aslam.

Writing – review & editing: Muhammad Aslam, Jean-Claude Malela-Majjika, Sandile C. Shongwe.

References

1. Montgomery DC, Introduction to Statistical Quality Control, 6th Edition, John Wiley & Sons, Hoboken, New Jersey; 2009.
2. Lucas JM, Saccucci MS. Exponentially weighted moving average control schemes: Properties and enhancements. *Technometrics*. 1990; 32(1): 1–12. <https://doi.org/10.1080/00401706.1990.10484583>
3. Zhao YI, Tsung F, Wang F. Dual CUSUM control schemes for detecting a range of mean shifts. *IIE Transactions*. 2005; 37(11): 1047–1057. <https://doi.org/10.1080/07408170500232321>.
4. Li Z, Wang Z. Adaptive CUSUM of the Q chart. *International Journal of Production Research*. 2010; 48(5): 1287–1301. <https://doi.org/10.1080/00207540802484937>.
5. Shafqat A, Huang Z, Aslam M, and Nawaz MS. A Nonparametric repetitive sampling DEWMA control chart based on linear prediction. *IEEE Access*; 2020; 8: 74977–74990. <https://doi.org/10.1109/ACCESS.2020.2989132>.
6. Haq A. An improved mean deviation exponentially weighted moving average control chart to monitor process dispersion under ranked set sampling. *Journal of Statistical Computation and Simulation*. 2014; 84(9), 2011–2024 <https://doi.org/10.1080/00949655.2013.780059>
7. Haq A, Brown J, and Moltchanova E. New exponentially weighted moving average control charts for monitoring process mean and process dispersion. *Quality and Reliability Engineering International*. 2015; 31(5): 877–901. <https://doi.org/10.1002/qre.1646>.
8. Haq A, Brown J, Moltchanova E, Al-Omari AI. Effect of measurement error on exponentially weighted moving average control charts under ranked set sampling schemes. *Journal of Statistical Computation and Simulation*. 2015; 85(6): 1224–1246. <https://doi.org/10.1080/00949655.2013.873040>.

9. Sanusi RA, Riaz M, Adegoke NA, Xie M. An EWMA monitoring scheme with a single auxiliary variable for industrial processes. *Computers & Industrial Engineering*. 2017; 114: 1–10. <https://doi.org/10.1016/j.cie.2017.10.001>.
10. Shafqat A, Huang Z, Aslam M. Design of X-bar control chart based on Inverse Rayleigh Distribution under repetitive group sampling. *Ain Shams Engineering Journal*. 2020; <https://doi.org/10.1016/j.asej.2020.06.001>.
11. Shafqat A., Hussain J., Al-Nasser A. D., and Aslam M. Attribute control chart for some popular distributions. *Communications in Statistics—Theory and Methods*. 2018; 47(8):1978–1988. <https://doi.org/10.1080/03610926.2017.1335414>.
12. Khademi M, Amirzadeh V. Fuzzy rules for fuzzy x and r control charts. *Iranian Journal of Fuzzy Systems*. 2014; 11(5): 55–66. <https://doi.org/10.22111/IJFS.2014.1722>.
13. Sabegh MHZ, Mirzazadeh A, Salehian S, Weber GW. A literature review on the fuzzy control chart: classifications & analysis. *International Journal of Supply and Operations Management*. 2014; 1(2): 167–189. <https://doi.org/10.22034/2014.2.03>.
14. Senturk S, Erginel N. Development of fuzzy $\bar{\bar{X}} - \bar{R}$ and $\bar{\bar{X}} - \bar{S}$ control charts using α -cuts. *Information Sciences*. 2009; 179(10):1542–1551. <https://doi.org/10.1016/j.ins.2008.09.022>.
15. Faraz A, Kazemzadeh RB, Moghadam MB, Bazdar A. Constructing a fuzzy Shewhart control chart for variables when uncertainty and randomness are combined. *Quality & Quantity*, 2010; 44: 905–914. <https://doi.org/10.1007/s11135-009-9244-9>.
16. Smarandache F. Neutrosophic Logic—A generalization of the intuitionistic fuzzy logic. *SSRN Electronic Journal*, 2016. <https://dx.doi.org/10.2139/ssrn.2721587>.
17. Smarandache F. Introduction to Neutrosophic Statistics, Sitech & Education Publishing, Craiova, Romania & Ohio, USA; 2014.
18. Khalid HE, Essa AK. Introduction to Neutrosophic Statistics, the translated Arabic version, Pons Publishing House, Brussels, Belgium, 2020.
19. Morán JCS, Chuga JFE, Collaguazo WMA, Gudiño CWM. Neutrosophic statistics applied to the analysis of socially responsible participation in the community. *Neutrosophic Sets and Systems*, 2019; 26:19–28. <https://doi.org/10.5281/zenodo.3244232>.
20. Maldonado PAC, Martinez YP, Valverde GSE, Erazo JDI. Neutrosophic statistics methods applied to demonstrate the extra-contractual liability of the state from the Administrative Organic Code. *Neutrosophic Sets and Systems*, 2019; 26:29–34. <https://doi.org/10.5281/zenodo.3244262>.
21. Carballido RM, Paronyan H, Matos MA, Molina ALS. Neutrosophic statistics applied to demonstrate the importance of humanistic and higher education components in students of legal careers. *Neutrosophic Sets and Systems*, 2019; 26:174–180. <https://doi.org/10.5281/zenodo.3244848>
22. Panthong C, Pongpullonsak A. Non-normality and the fuzzy theory for variable parameters \bar{X} control charts. *Thai Journal of Mathematics*, 2016; 14(1):203–213.
23. Pereira P, Seghatchian J, Caldeira B, Xavier S, de Sousa G. Statistical methods to the control of the production of blood components: Principles and control charts for variables. *Transfusion and Apheresis Science*, 2018; 57(1):132–142. <https://doi.org/10.1016/j.transci.2018.02.022> PMID: 29526479
24. Aslam M, Bantan RAR, Khan N. Design of a new attribute control chart under neutrosophic statistics. *International Journal of Fuzzy Systems*, 2019; 21:433–440. <https://doi.org/10.1007/s40815-018-0577-1>.
25. Aslam M, Rao GS, Shafqat A, Ahmad L, Sherwani RAK. Monitoring circuit boards products in the presence of indeterminacy. *Measurement*, 2021; 168:108404. <https://doi.org/10.1016/j.measurement.2020.108404>.
26. Khan Z, Gulistan M, Hashim R, Yaqoob N, Chammam W. Design of S-control chart for neutrosophic data: An application to manufacturing industry. *Journal of Intelligent & Fuzzy Systems*. 2020; 38(4): 4743–4751. <https://doi.org/10.3233/JIFS-191439>.
27. Aslam M. Attribute Control Chart Using the Repetitive Sampling under Neutrosophic System. *IEEE Access*, 2019; 7:15367–15374. <https://doi.org/10.1109/ACCESS.2019.2895162>.
28. Aslam M. Control chart for variance using repetitive sampling under neutrosophic statistical interval system. *IEEE Access*, 2019; 7: 25253–25262. <https://doi.org/10.1109/ACCESS.2019.2899020>.
29. Page ES. Continuous inspection schemes. *Biometrika*, 1954; 41(1–2): 100–115. <https://doi.org/10.1093/biomet/41.1-2.100>.